Published OnlineFirst May 8, 2017; DOI: 10.1158/0008-5472.CAN-16-2797

Molecular and Cellular Pathobiology

Cancer Research

TWIST1-WDR5-*Hottip* Regulates *Hoxa9* Chromatin to Facilitate Prostate Cancer Metastasis

Reem Malek[1], Rajendra P. Gajula[1], Russell D. Williams[1], Belinda Nghiem[2], Brian W. Simons[3], Katriana Nugent[1], Hailun Wang[1], Kekoa Taparra[1,4], Ghali Lemtiri-Chlieh[1], Arum R. Yoon[5], Lawrence True[6], Steven S. An[5,7,8], Theodore L. DeWeese[1,3,7], Ashley E. Ross[3,7], Edward M. Schaeffer[3,7], Kenneth J. Pienta[3,4,7], Paula J. Hurley[3,4,7], Colm Morrissey[2], and Phuoc T. Tran[1,3,4,7]

Abstract

TWIST1 is a transcription factor critical for development that can promote prostate cancer metastasis. During embryonic development, TWIST1 and HOXA9 are coexpressed in mouse prostate and then silenced postnatally. Here we report that TWIST1 and HOXA9 coexpression are reactivated in mouse and human primary prostate tumors and are further enriched in human metastases, correlating with survival. TWIST1 formed a complex with WDR5 and the lncRNA Hottip/HOTTIP, members of the MLL/COMPASS–like H3K4 methylases, which regulate chromatin in the Hox/HOX cluster during development. TWIST1 overexpression led to coenrichment of TWIST1 and WDR5 as well as increased H3K4me3 chromatin at the Hoxa9/HOXA9 promoter, which was dependent on WDR5. Expression of WDR5 and Hottip/HOTTIP was also required for TWIST1-induced upregulation of HOXA9 and aggressive cellular phenotypes such as invasion and migration. Pharmacologic inhibition of HOXA9 prevented TWIST1-induced aggressive prostate cancer cellular phenotypes *in vitro* and metastasis *in vivo*. This study demonstrates a novel mechanism by which TWIST1 regulates chromatin and gene expression by cooperating with the COMPASS-like complex to increase H3K4 trimethylation at target gene promoters. Our findings highlight a TWIST1–HOXA9 embryonic prostate developmental program that is reactivated during prostate cancer metastasis and is therapeutically targetable. *Cancer Res; 77(12); 3181–93. ©2017 AACR.*

Introduction

Prostate cancer is the most commonly diagnosed cancer for men, and leads to the second most cancer-related deaths in the United States (1). Prostate cancer natural history disease progression suggests that the largest therapeutic gains could be made by better understanding the progression of localized to metastatic disease (2).

Previous studies have implicated the epithelial–mesenchymal transition (EMT) transcription factor, TWIST1, in human prostate tumor pathogenesis correlating it with increased disease aggressiveness (3, 4). TWIST1 can induce prometastatic behaviors in prostate cancer cells (5) that is, in part, mediated by the homeobox protein HOXA9 (6).

Homeobox transcription factors, like HOXA9, are crucial to body plan organization during development, and are tightly regulated both spatially and temporally (7). The expression of genes in this cluster is regulated epigenetically that include critical alterations in chromatin methylation (8). *HOX* gene products also play a role in progression of cancer with *HOXA9* and *HOXB13* being the most commonly altered *HOX* genes in solid tumors (9). While the contribution of HOXA9 overexpression in leukemia, specifically AML, has been firmly established (10), the role of HOXA9 in prostate cancer progression has not been well documented.

In normal tissue, the *Hox*/*HOX* cluster of genes is regulated at the chromatin level (11) by the complex of proteins associated with SET1 (COMPASS)-like complex that involves several mixed lineage leukemia (*MLL*) gene products (homolog of yeast Set1), the scaffolding protein, WDR5, and the long noncoding RNA (lncRNA), *HOTTIP* (12). COMPASS-like complex activates gene expression by methylation of histone 3 on lysine 4 (H3K4; ref. 13). Although, first discovered in leukemias (14), *KMT2* have since been found to be among the most frequently mutated genes in human cancer (15). *KMT2D*/*MLL2* mutations distinguish the transition from localized to lethal metastatic castration-resistant prostate cancer (16). In addition,

[1]Department of Radiation Oncology and Molecular Radiation Sciences, Sidney Kimmel Comprehensive Cancer Center, Johns Hopkins University School of Medicine, Baltimore, Maryland. [2]Department of Urology, University of Washington, Seattle, Washington. [3]Department of Urology, Johns Hopkins University School of Medicine, Baltimore, Maryland. [4]Cellular and Molecular Medicine Program, Johns Hopkins University School of Medicine, Baltimore, Maryland. [5]Department of Environmental Health Sciences, Johns Hopkins University Bloomberg School of Public Health, Baltimore, Maryland. [6]Department of Pathology, University of Washington, Seattle, Washington. [7]Department of Oncology, Sidney Kimmel Comprehensive Cancer Center, Johns Hopkins University School of Medicine, Baltimore, Maryland. [8]Department of Chemical and Biomolecular Engineering, Johns Hopkins University, Baltimore, Maryland.

Note: Supplementary data for this article are available at Cancer Research Online (http://cancerres.aacrjournals.org/).

R. Malek, R.P. Gajula, and R.D. Williams contributed equally to this article.

Corresponding Author: Phuoc T. Tran, Sidney Kimmel Comprehensive Cancer Center, Johns Hopkins Hospital, 1550 Orleans Street, CRB2 Rm 406, Baltimore, MD 21231. Phone: 410-614-3880; Fax: 410-502-1419; E-mail: tranp@jhmi.edu

doi: 10.1158/0008-5472.CAN-16-2797

Published OnlineFirst May 8, 2017; DOI: 10.1158/0008-5472.CAN-16-2797

COMPASS-like H3K4 methyltransferase (HMT) complexes physically associate with androgen receptor (AR) and have been shown to be required for direct AR target gene expression and prostate cancer growth (17).

In this study, we show that *TWIST1* and *HOXA9* were coover-expressed in prostate cancer tumors and metastases. We demonstrated an interaction between TWIST1 and members of the COMPASS-like complex, WDR5 and *Hottip*/*HOTTIP* in regulation of *Hoxa9*/*HOXA9* expression. Finally, we showed pharmacologic inhibition of HOXA9 could mitigate TWIST1-induced prometastatic behaviors *in vitro* and metastasis *in vivo*.

Materials and Methods

Plasmids, antibodies, and reagents

pBABE-TWIST1-puro was used to construct the Twist1DQD mutant as described previously (5, 18) using the QuikChange Site-Directed Mutagenesis Kit (Stratagene) and confirmed by sequencing. The following antibodies were used: Twist (Twist2C1a, sc-81417; Santa Cruz Biotechnology), E-cadherin (ab53033; Abcam), vimentin (ab92547; Abcam), ZO-1 (5406; Cell Signaling Technology), β-actin (A5316; Santa Cruz Biotechnology), WDR5 (ab56919; Abcam), H3K4me3 (ab8580; Abcam), H3K27me3 (ab6002; Abcam), and horseradish peroxidase–conjugated secondary antibodies (Invitrogen).

Cell lines and culture conditions

The cell lines used in this study, PC3, K562, MOLM-13, and HEK293, were obtained from ATCC. Myc-CaP cell line was a kind gift from Dr. John Isaacs (Johns Hopkins University, Baltimore, MD). All cell lines were obtained between 2011 and 2014 and authenticated using short tandem repeat analysis. All the cell lines were expanded and frozen immediately after receipt. The cumulative culture length of the cells was less than 6 months after recovery. Early passage cells were used for all experiments and routinely tested for mycoplasma. Cells were maintained as described by ATCC.

Microarray data acquisition and analysis

Microarrays and bioinformatics analysis were performed previously (5). Details provided in Supplementary Methods. The microarray data have been deposited to the Gene Expression Omnibus (GSE500002).

Retroviral experiments

The shRNA constructs against mouse *Hoxa9*, human *HOXA9*, mouse *Wdr5*, and human *WDR5* were used according to the manufacturer's instructions (OriGene). Cells were transduced with pGFP-V-RS–based shRNA constructs as described above or with scrambled control vector for two successive times over a 36-hour period followed by selection with 1 mg/mL puromycin and passaged once until 80% confluent.

TALEN genetic knockout

TALEN genetic editing to knock out *WDR5* in PC3 cells was accomplished using a TALEN-FastTALE kit (Allele Biotechnology) according to the manufacturer's instructions.

Patient tissue acquisition

Samples for IHC were obtained from patients who died of metastatic CRPC and who signed written informed consent for a rapid autopsy performed within 8 hours of death, under the aegis of the Prostate Cancer Donor Program at the University of Washington. The institutional review board at the University of Washington (Seattle, WA) approved the study. Bone metastases were formalin fixed, decalcified in 10% formic acid and embedded in paraffin.

IHC, immunofluorescence, and Western blotting

IHC, immunofluorescence, and Western blotting were conducted as described previously (19). Details are provided in Supplementary Methods.

SYBR-Green quantitative RT-PCR and prostate cancer cDNA arrays

The iTaq Universal SYBR Green Master Mix (Bio-Rad) was used according to the manufacturer's instructions and as described previously (6). Human normal prostate and prostate cancer qPCR tissue arrays were purchased from OriGene.

Cell behavior assessment

For wound-healing migration assay, two-dimensional migration assays were conducted using a scratch/wound model as described previously (6). For Matrigel invasion assay, invasion potential was assessed using Chemicon cell invasion assay kit (Millipore) as directed by the manufacturer. Soft agar colony formation assays were performed as described previously (20). Anoikis resistance was measured as described previously (21). Cell stiffness assay, magnetic twisting cytometry (MTC) was used to measure mechanical properties of the cytoskeleton as described previously (22, 23). Details are given in Supplementary Methods.

Protein coimmunoprecipitation and RNA immunoprecipitation

Protein coimmunoprecipitation and RNA immunoprecipitation were performed as described previously (24). Details are given in Supplementary Methods.

Chromatin immunoprecipitation and ChIP-re-ChIP

Chromatin immunoprecipitation (ChIP) was conducted using a SimpleChIP Enzymatic IP Kit (Cell Signaling Technology) according to the manufacturer's instructions. Details are given in Supplementary Methods.

Experimental lung metastasis assay

Myc-CaP cells stably overexpressing TWIST1 were treated with 10 nmol/L HXR9 or CXR9 for 24 hours before tail vein injection. One-hundred microliters of PBS containing 5×10^5 cells were injected into athymic nude mice via the tail vein. After 4 weeks, the mice were sacrificed, and necropsies were performed to score surface lung tumors and extrathoracic metastases as described previously (6).

Statistical analysis

Statistical analysis was carried out using GraphPad Prism v5.04 (GraphPad Software). Paired comparisons of the average were tested using the Mann–Whitney test. Paired comparisons of the frequency of an event were performed by contingency tables with the Fisher exact test (*, $P < 0.05$; **, $P < 0.01$; and ***, $P < 0.001$; throughout this study).

Published OnlineFirst May 8, 2017; DOI: 10.1158/0008-5472.CAN-16-2797

Results

Bioinformatic analyses identified HOXA9 as a putative downstream target responsible for TWIST1-induced prometastatic behaviors

We reported on TWIST1 structure–function studies and the effects of overexpression of mouse *Twist1* mutants on the induction of TWIST1-dependent aggressive cellular prometastatic phenotypes *in vitro* and *in vivo* (Fig. 1A; refs. 5, 6). Global gene expression analyses were performed on Myc-CaP cells expressing wild-type TWIST1, TWIST1-F191G, which does not induce a metastatic phenotype, and TWIST1-DQD, which induces a more pronounced metastatic phenotype (Fig. 1B). Subtractive gene expression analysis identified genes whose expression was significantly altered in cells expressing wild-type TWIST1, but not in cells expressing TWIST1-F191G, and genes whose expression was significantly altered in cells expressing TWIST1-DQD but not in cells expressing wild-type TWIST1 (Fig. 1C). Resultant gene sets were associated with increasing intensity of TWIST1-induced EMT phenotypes (Fig. 1D).

Gene-set enrichment analysis (GSEA) was performed on both sets of genes, and in both cases, gene sets representing target genes of constitutively active HOXA9 fusion proteins (25, 26) were significantly overrepresented (Supplementary Table S3). This led us to hypothesize that HOXA9 activation was downstream of TWIST1 and was responsible for enforcing TWIST1-induced prometastatic phenotypes (Fig. 1D).

TWIST1 and HOXA9 are coexpressed in the developing embryonic mouse prostate and reactivated in mouse prostate tumors

Limited mRNA expression data suggest that the posterior *Hox* cluster gene *Hoxa9* is expressed transiently in the prostate following rodent birth and then expression is suppressed in adulthood (27). The role of TWIST1 and HOXA9 during prostate development is unknown. We observed by qRT-PCR of bulk fetal prostate tissue that *Twist1* and *Hoxa9* were both coexpressed with expression peaking during periods of early prostate bud invasion (E17.5 and E18.5, respectively), and then nadiring after birth at day P5 (Fig. 2A). The adult prostate is derived from both the embryonic urogenital mesenchyme (UGM) and urogenital epithelium (UGE). To define the cell types expressing and subcellular localization of TWIST1 and HOXA9, we examined developmental protein expression in the mouse developing prostate using IHC. Concordant with the temporal mRNA expression, TWIST1 and

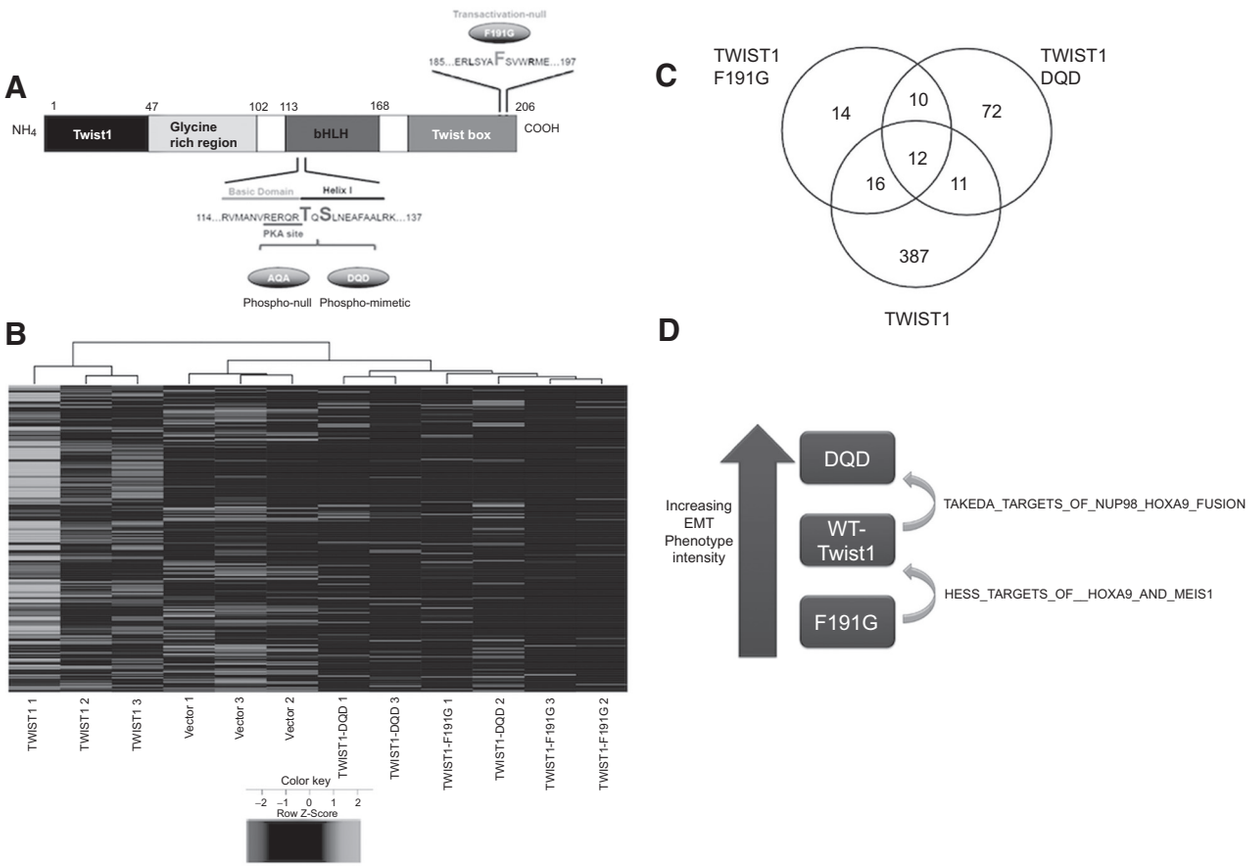

Figure 1.

Gene expression profiling of TWIST1 structure–function mutants revealed *HOXA9* as a downstream target. **A,** Schematic of TWIST1 structure, T125D and S127D site-specific mutant, TWIST1-DQD, TWIST1-F191G. **B,** Unsupervised hierarchal clustering heatmap visualization of gene expression differentially regulated by vector, TWIST1, TWIST1-DQD, and TWIST1-F191G. **C,** Venn diagram represents significantly differentially expressed genes between Myc-CaP-TWIST1 and TWIST1 mutants. **D,** GSEA analysis revealed that *HOXA9* gene signatures were correlated with an increased EMT and metastatic phenotype.

Published OnlineFirst May 8, 2017; DOI: 10.1158/0008-5472.CAN-16-2797

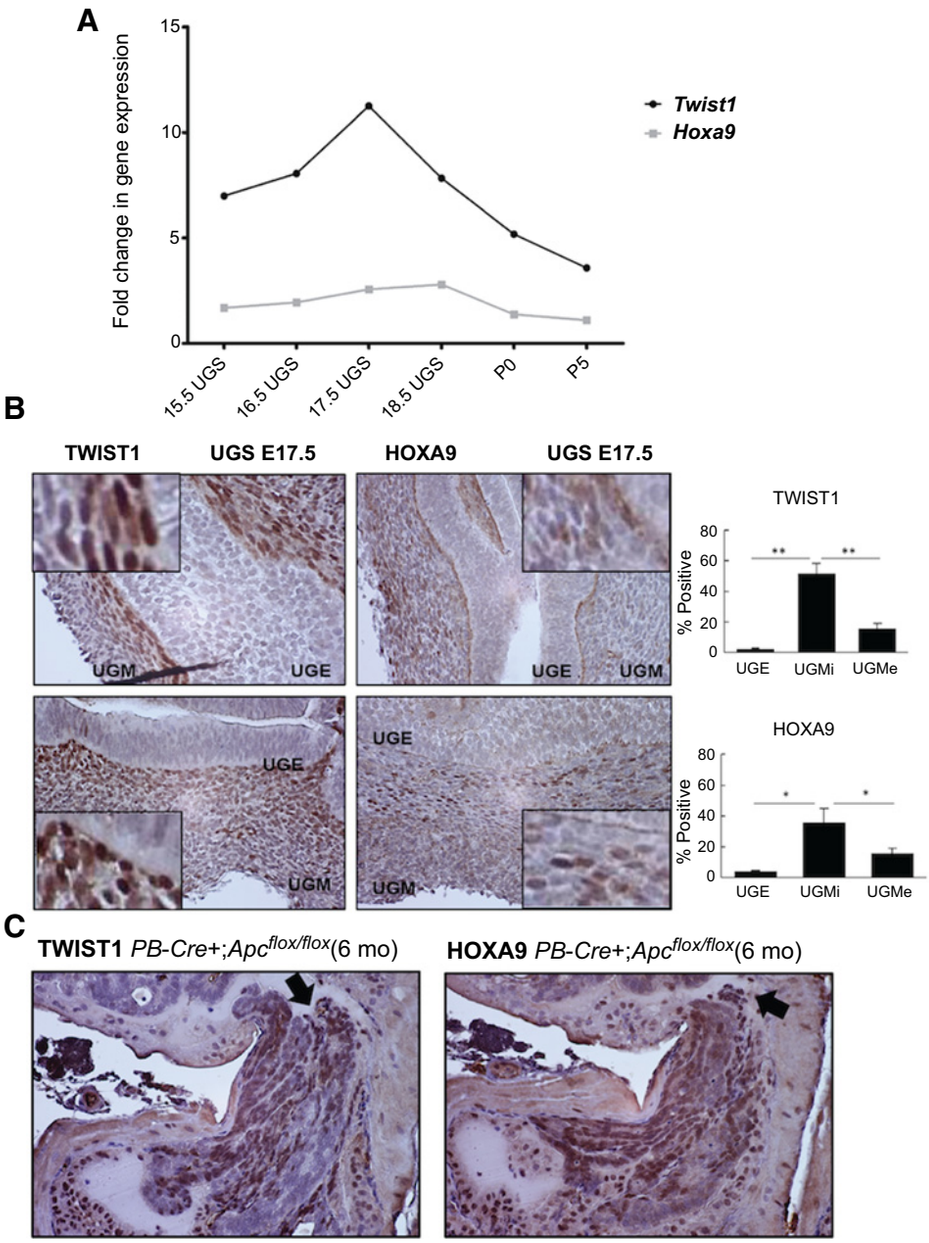

Figure 2.
TWIST1 and HOXA9 are coexpressed in the developing mouse prostate and in autochthonous prostate neoplastic lesions. **A**, *Twist1* and *Hoxa9* gene expression by qPCR in E15.5-E18.5 UGS and P0, P5 developing prostate ($n = 3$–6 embryos-pups/time point/gene, Pearson correlation coefficient ($R^2 = 0.82$). Normalized to expression level at P35. **B**, TWIST1 and HOXA9 IHC on serial sections of E17.5 UGS from wild-type mice in cells at the urogenital mesenchyme (UGM)–urogenital epithelium (UGE) interface. UGMi, section of the UGM closest to the UGE interface; UGMe, section of the UGM toward the edge. Graphs represent percentage positive cells ($n = 4$ embryos). *, $P < 0.05$; **, $P < 0.01$. **C**, TWIST1 and HOXA9 IHC on adjacent serial sections of prostate tissue from *probasin (PB)-Cre; Apc$^{flox/flox}$* mice with prostate neoplasia ($n = 2$). Arrows, TWIST and HOXA9 coexpression in the same cell types.

HOXA9 showed predominantly nuclear peak individual expression and coexpression during E17.5 in cells from the developing UGM, with highest coexpression among cells along the UGM–UGE interface (Fig. 2B). In agreement with the mRNA expression data, we observed a steady decrease in TWIST1 expression at P0 and P5 with no observable TWIST1 expression at time-points thereafter (Supplementary Fig. S1). Overall, this observation suggests that HOXA9 may be a target of TWIST1 during mammalian prostate development.

TWIST1 expression is often aberrantly reactivated in human cancers including prostate cancer (3, 6, 28), but data on expression of HOXA9 in prostate cancer is lacking. We did not observe appreciable IHC staining for either TWIST1 or HOXA9 in prostate epithelial cells in tumors from the TRAMP (29), Hi-Myc (30), or *Pten*$^{-/-}$ (31) transgenic mouse models of prostate cancer or the adult wild-type prostate (Supplementary Fig. S2 and S5B). However, in the *PB-Cre+;Apc$^{flox/flox}$* mouse model of prostate cancer (32), we observed cooverexpression of TWIST1 and HOXA9 in neoplastic prostate epithelial cells (Fig. 2C). Thus, we found that coexpression of TWIST1 and HOXA9 could be reactivated in at least one model of prostate epithelial tumorigenesis.

TWIST1 and HOXA9 are cooverexpressed in human prostate cancer and correlated with poor patient survival

Analysis of publicly available prostate cancer patient gene expression data through Oncomine (www.oncomine.org) showed that *HOXA9* trended toward overexpression overall in several different studies (Fig. 3A; $n = 700$ prostate cancers versus

Published OnlineFirst May 8, 2017; DOI: 10.1158/0008-5472.CAN-16-2797

$n = 313$ normal prostate, $P = 0.095$) similar to TWIST1 (6). *TWIST1* and *HOXA9* were shown to be trending toward cooverexpression in primary prostate cancer, 13% and 21%, respectively ($n = 131$, $P = 0.12$). Interestingly, coamplification/overexpression cases were significantly enriched when examining metastases [42% alteration for *TWIST1* and 32% for *HOXA9*, $n = 19$, $P = 0.024$ Fisher exact test; MKSCC Prostate Adenocarcinoma dataset (33)] using the cBio portal (Fig. 3B; refs. 34, 35). We validated that *HOXA9* was overexpressed in primary prostate cancer (Fig. 3C, $n = 91$, $P < 0.001$) and that *TWIST1* and *HOXA9* were both found to be overexpressed in primary prostate cancer compared with normal prostate in another independent patient dataset (Origene TissueScan qPCR array; Fig. 3C and D). In addition, samples with high *TWIST1* expression were disproportionately likely to have high *HOXA9* expression (Fig. 3E). In a third independent patient dataset, we found that *TWIST1* and *HOXA9* were coamplified in metastatic prostate cancer and *HOXA9* amplification alone or when considered with *TWIST1* amplification was correlated with worse overall patient survival (Michigan Prostate Adenocarcinoma dataset, Fig. 3F; Supplementary Fig. S3.; $n = 61$, both $P < 0.024$). Finally, using prostate cancer samples from a prospectively collected rapid autopsy series, we showed by IHC that TWIST1 and HOXA9 were colocalized in the nucleus of tumor cells in prostate cancer primary tumors ($n = 3$) and bone metastases ($n = 6$ patients, Fig. 3G and H; Supplementary Fig. S4A and S4B). Collectively, multiple independent human prostate cancer cohorts showed that *TWIST1* and *HOXA9* are dysregulated together at the genetic level and also cooverexpressed at the protein level in a subset of prostate cancer, particularly metastatic samples that are correlated with poor patient survival.

We have previously shown that HOXA9 was partially required for TWIST1-induced prometastatic behaviors *in vitro* (6). We found that stable overexpression of human *HOXA9* alone in Myc-CaP and PC3 cells (Supplementary Fig. S6A and S6B)

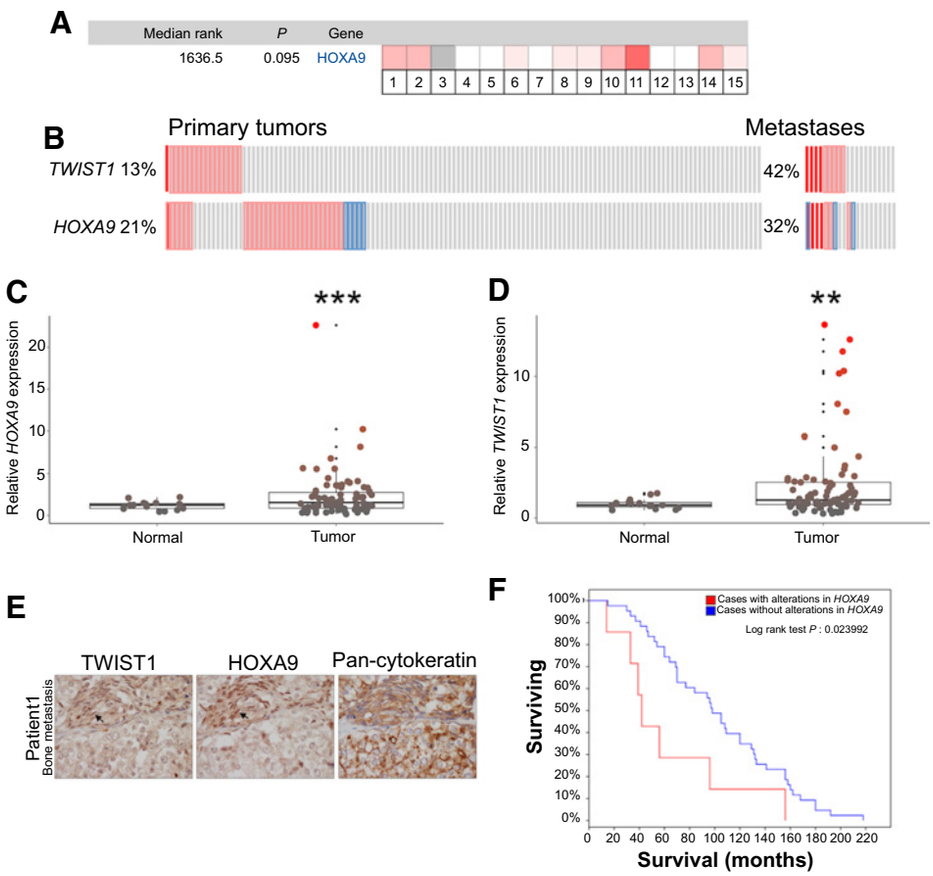

Figure 3.

TWIST1 and HOXA9 are cooverexpressed in metastatic prostate cancer and correlate with poor survival. **A,** *HOXA9* trended toward overexpression in several sets of prostate adenocarcinoma gene expression data analyzed using Oncomine ($n = 15$ independent microarray datasets equaling 700 primary prostate cancer samples and 313 normal prostates; $P = 0.095$). **B,** *TWIST1* and *HOXA9* trended toward coamplification/overexpression in a subset of primary tumors from patients with prostate adenocarcinoma using the cBio portal (MKSCC Prostate Adenocarcinoma dataset, $n = 131$ patient samples; $P = 0.12$). **C** and **D,** *HOXA9* and *TWIST* expression in a commercially available cDNA array of prostate cancer tissue samples compared with normal prostate tissue ($n = 91$ prostate cancer patient samples; Mann–Whitney *t* test, **, $P < 0.01$ and ***, $P < 0.001$). **E,** *TWIST1* and *HOXA9* cooverexpression is enriched in prostate adenocarcinoma metastases (Fisher exact test, $n = 19$, $P = 0.024$). **F,** Amplification of *HOXA9* is associated with shorter survival in patients with prostate adenocarcinoma, analyzed from cBio (Michigan Prostate Adenocarcinoma dataset, $n = 61$ patients, $P < 0.024$, log-rank test). **G** and **H,** Representative example of TWIST1, HOXA9, and IgG/pan-cytokeratin on adjacent serial sections of a primary and bone metastasis from prostate adenocarcinoma patients. Arrows highlight TWIST and HOXA9 coexpression in the nuclei of tumor cells.

Published OnlineFirst May 8, 2017; DOI: 10.1158/0008-5472.CAN-16-2797

enforced a partial EMT, increased migratory potential (Supplementary Fig. S6C and S6D, all comparisons $P < 0.01$), invasiveness (Supplementary Fig. S6E and S6F, $P < 0.05$), anoikis resistance (Supplementary Fig. S6G and S6H, $P < 0.05$), and radiation resistance (Supplementary Fig. S6K and S6L, $P < 0.05$). These data suggest that HOXA9 alone is sufficient to induce many prometastatic behaviors *in vitro* and is partially required for TWIST1-induced prometastatic behaviors (6).

TWIST1 interacts with members of the MLL/COMPASS–like complex

Hoxa9 expression is activated during development by MLL/COMPASS-like–dependent methylation of promoter histones. It was recently shown that TWIST1 can lead to changes in the epigenetic landscape involving DNA as well as histone modifications (36). One possibility is that TWIST1 may modulate expression of *Hoxa9* epigenetically through interaction with a COMPASS-like complex. In the MSKCC Prostate Adenocarcinoma dataset (34, 35), *TWIST1* was cooverexpressed with a gene encoding a member of the COMPASS-like HMT complex, *KMT2D* (*MLL2/ALR/MLL4*) in prostate cancer metastases (Fig. 4A, $n = 19$, $P = 0.049$ by Fisher exact test). TWIST1 has been shown to bind WDR5 under conditions of hypoxia-induced EMT (37). To test whether TWIST1 bound WDR5 in prostate cancer cells and under normoxic conditions, we performed coimmunoprecipitation experiments on extracts from HEK293 embryonic kidney cells, Myc-CaP and PC3 prostate cancer cells that stably overexpressed TWIST1 and also in K562 leukemia cells that have intrinsically high TWIST1 expression. Anti-TWIST1 antibody pulled down WDR5 in all cell lines, but PC3 (data not shown), and we also observed the reciprocal interaction when cell lysates were coimmunoprecipitated with anti-WDR5 antibody and probed for TWIST1 (Fig. 4B). These results indicate TWIST1 and WDR5 interact with each other in cancer cells under normoxic conditions and this interaction may be in the context of the larger COMPASS-like HMT complex.

We investigated how TWIST1 influences another component of the MLL/COMPASS-like complex that regulates the *Hox* cluster during development, *Hottip*, an lncRNA that directly binds to the complex and directs it to sites in the *Hox* cluster (24). We found that HOXA9 overexpression in Myc-CaP and PC3 cells led to an increase in *Hottip*/*HOTTIP* expression

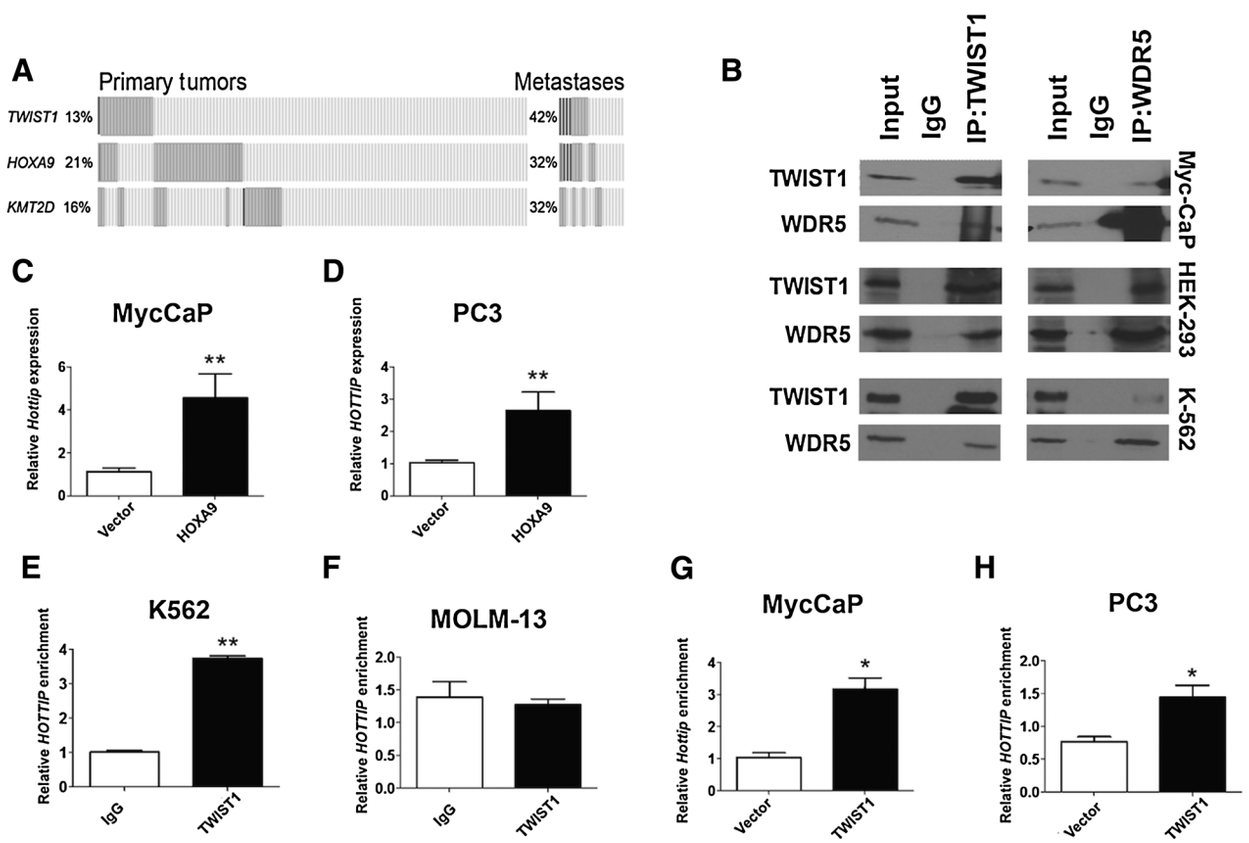

Figure 4.

TWIST1 interacts with the components of the MLL/COMPASS–like complex WDR5 and *Hottip*/*HOTTIP*. **A,** Gene encoding MLL2, *KMT2D,* showed significant cooverexpression with *TWIST1* in the MKSCC Prostate Adenocarcinoma dataset in prostate cancer metastases (Fisher exact test, $n = 19$, $P = 0.049$). **B,** TWIST1 and WDR5 pulldown by immunoprecipitation in HEK-293, Myc-CaP-TWIST1, and in K-562 cells compared with IgG control. **C** and **D,** Expression of *Hottip/HOTTIP* in Myc-CaP-HOXA9 and PC3-HOXA9 cells compared with vector control ($n = 3$–4; Mann–Whitney *t* test, **, $P < 0.01$; ±SEM). Coimmunoprecipitation of *HOTTIP* with TWIST1 in K562 (**E**), but not in MOLM-13 cells ($n \geq 2$; Mann–Whitney *t* test, **, $P < 0.01$; ±SEM; **F**). Coimmunoprecipitation *of hottip/*HOTTIP with TWIST1 in Myc-CaP-TWIST1 cells (**G**) and PC3-TWIST1 cells (**H**) compared with isogenic vector control cells ($n \geq 3$; Mann–Whitney *t* test, *, $P < 0.05$; ±SEM).

Published OnlineFirst May 8, 2017; DOI: 10.1158/0008-5472.CAN-16-2797

(Fig. 4C and D). To determine whether the TWIST1–WDR5 complex also contained *Hottip*/*HOTTIP*, we performed RNA immunoprecipitation (RIP) experiments using anti-TWIST1 antibody. In K562 leukemia cells, which have high endogenous TWIST1 expression, *HOTTIP* coprecipitated with TWIST1 (Fig. 4E, $P < 0.01$), but there was no detectable enrichment in MOLM-13 cells (Fig. 4F, $P > 0.05$), which do not express TWIST1. When we performed RIP experiments using anti-TWIST1 antibody in lysates of Myc-CaP and PC3 cells over-expressing TWIST1, we found significant enrichment of *Hottip*/*HOTTIP* (Fig. 4G and H, $P < 0.05$) as compared with vector controls. Overall, our results show that TWIST1 can interact with multiple members of the COMPASS-like HMT complex including the invariant component, WDR5, and the lncRNA, *Hottip*/*HOTTIP*. This physical interaction is highly suggestive that TWIST1-dependent upregulation of *Hoxa9* expression may be mediated by increasing the amount of activating H3K4 histone methylation at the *Hoxa9*/*HOXA9* promoter region.

Members of the MLL/COMPASS-like complex are required for TWIST1-mediated upregulation of Hoxa9 and induction of a metastatic phenotype

The active enzyme in the complex can be any one of several members of the MLL family (38), so genetic inhibition of any given member of the family may not have observable effects secondary to this redundancy. Therefore, we performed genetic knockdown of the invariant protein component WDR5 and the lncRNA *Hottip*/*HOTTIP*.

We showed that shRNA-mediated knockdown of *Wdr5* (Supplementary Fig. S7A) in Myc-CaP-TWIST1 cells led to a decrease in *Hoxa9* expression (Fig. 5A). Moreover, decreased *Wdr5* led to decreased migration potential (Fig. 5B; Supplementary Fig. S7B), invasiveness (Fig. 5C), resistance to radiation (Supplementary Fig. S7D), and anoikis resistance (Supplementary Fig. S7E) as compared with scrambled shRNA control cells. We used single-cell biophysical technique to measure cytoskeletal stiffness, magnetic twisting cytometry (MTC), and observed that

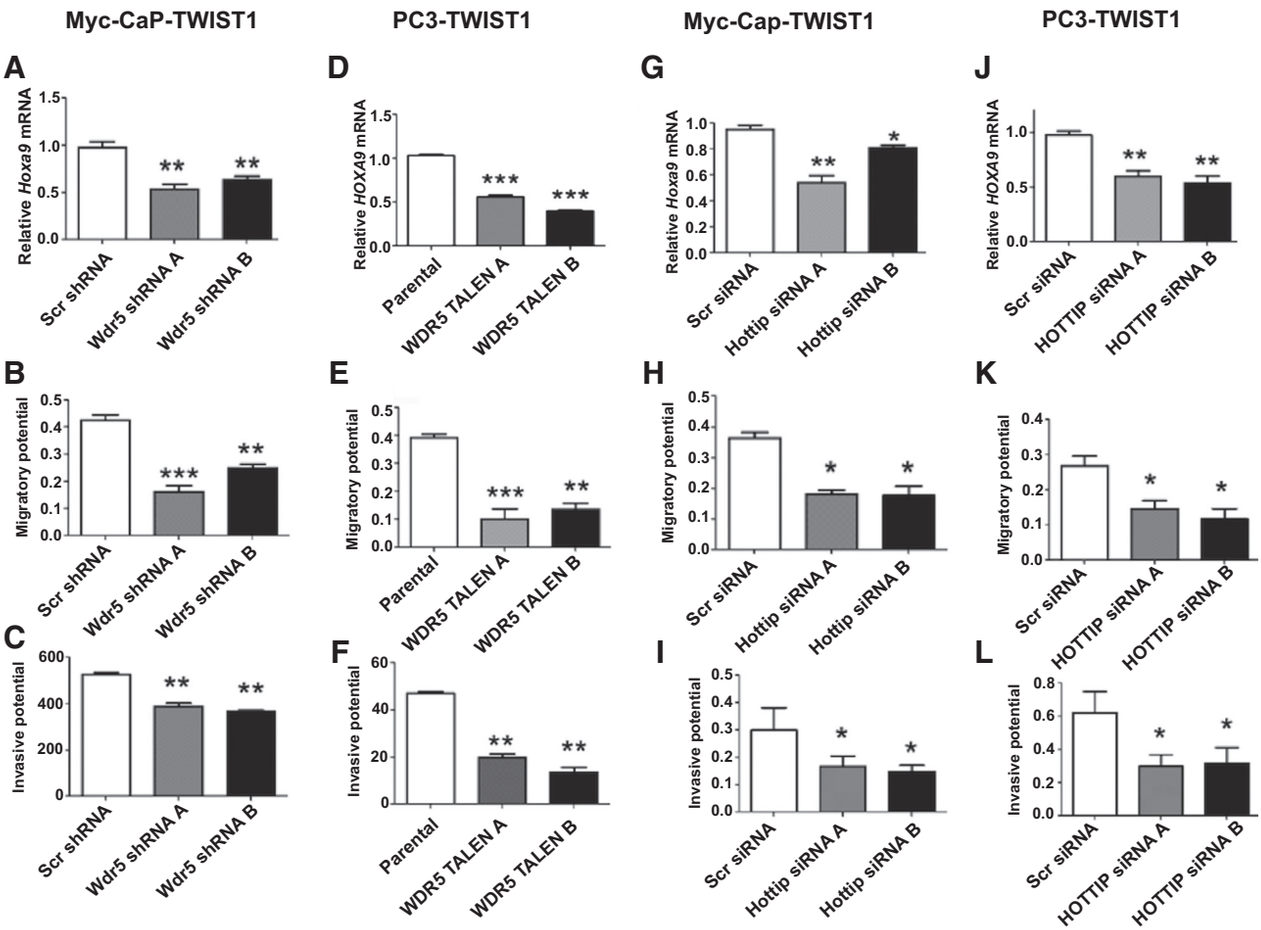

Figure 5.

WDR5 and *Hottip*/*HOTTIP* are required for TWIST1-mediated expression of HOXA9 and induction of prometastatic cellular phenotypes. **A,** *Wdr5* shRNA knockdown in Myc-CaP-TWIST1 cells reduced *Hoxa9* expression as shown by qPCR. Myc-CaP-TWIST1 cells with stable knockdown of *Wdr5* showed decreased migration (**B**) and invasion (**C**) through Matrigel compared with scrambled shRNA control. **D,** *WDR5* knockout by TALEN in PC3-TWIST1 cells decreased *HOXA9* expression. PC3-TWIST1 *WDR5* knockout cells had decreased cell migration (**E**) and invasion (**F**) through Matrigel cells compared with scrambled shRNA control. Knockdown of *Hottip*/*HOTTIP* by siRNA in Myc-CaP-TWIST1 (**G**) or PC3-TWIST1 cells (**J**), respectively, led to decreased *Hoxa9*/*HOXA9* mRNA. *Hottip* (**H**) or *HOTTIP* knockdown (**K**) led to decreased cell migration and invasion through Matrigel in Myc-CaP-TWIST1 and PC3-TWIST1 cells, respectively, compared to scrambled control (**I** and **L**). All were $n \geq 3$; Mann–Whitney *t* test, *, $P < 0.05$; **, $P < 0.01$; ***, $P < 0.001$; ±SEM.

Published OnlineFirst May 8, 2017; DOI: 10.1158/0008-5472.CAN-16-2797

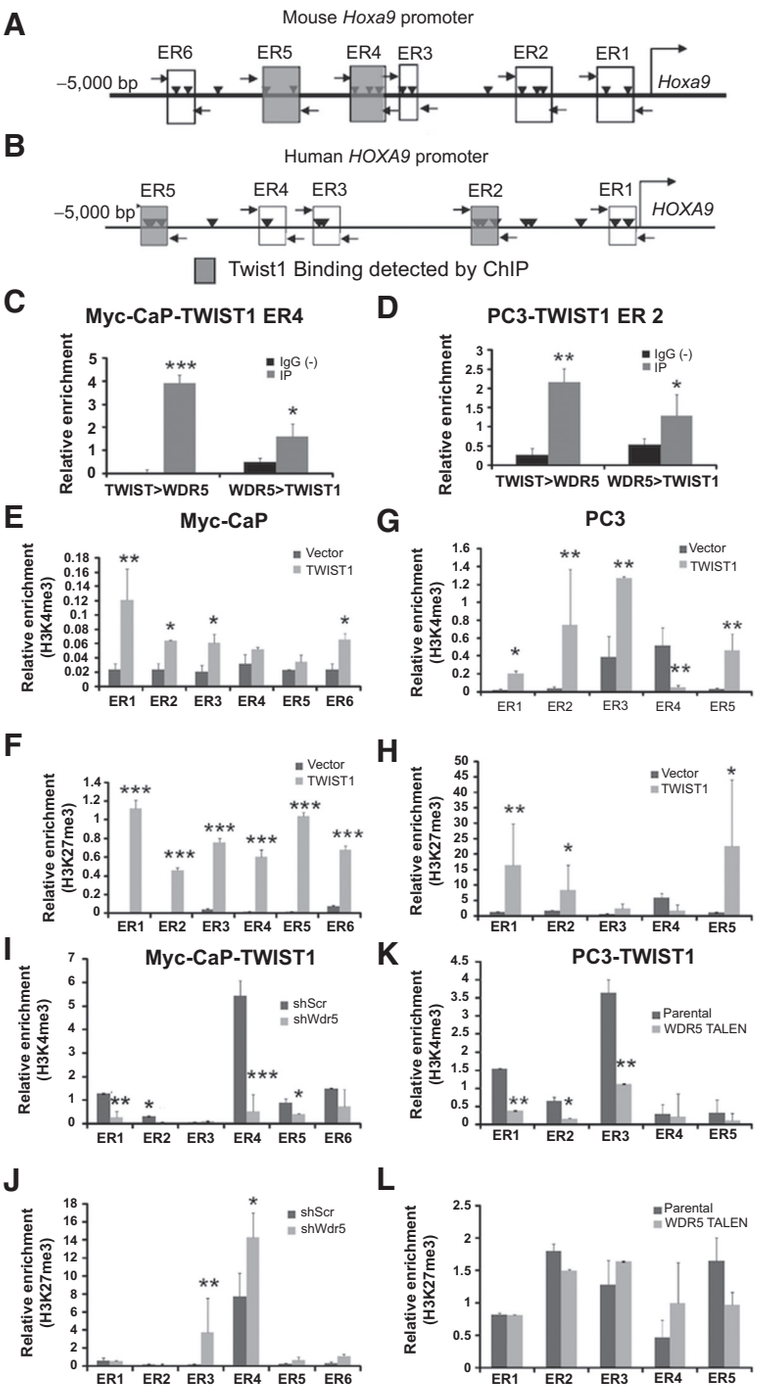

Figure 6.

TWIST1 interacts with WDR5 to increase H3K4me3 chromatin configuration of the *Hoxa9*/*HOXA9* promoter region. Schematic of the mouse *Hoxa9* (**A**) and human *HOXA9* (**B**) promoter. Rectangles represent E-box regions (ER) and shaded rectangles represent enrichment for TWIST1 binding. Arrowheads, individual E-box motifs. Horizontal arrows, ChIP primers. **C,** TWIST1 and WDR5 bind together at the *Hoxa9* promoter at ER4 by ChIP-re-ChIP in Myc-CaP-TWIST1 cells. **D,** TWIST1 and WDR5 also bind together at the human *HOXA9* promoter at ER2 by ChIP-re-ChIP in PC3-TWIST1 cells. ChIP with anti-H3K27me3 antibody showed increased H3K27me3 at several E-box regions in the *Hoxa9*/*HOXA9* promoter region in Myc-CaP-TWIST1 (**E**) and PC3-TWIST1 (**G**) cells compared with vector control cells. Similarly, ChIP with an anti-H3K4me3 antibody showed increased H3K4me3 at E-box regions in the *Hoxa9*/*HOXA9* promoter region of Myc-CaP-TWIST1 (**F**) and PC3-TWIST1 cells (**H**) compared with vector controls. **I** and **J,** *Wdr5* shRNA knockdown in Myc-CaP-TWIST1 cells decreased relative H3K4me3 enrichment observed with ChIP at the majority of E-box regions (**I**), but there was still some increased H3K27me3 observed in ER3 and ER4 of the *Hoxa9* promoter (**J**). **K** and **L,** *WDR5* knockout by TALEN in PC3-TWIST1 cells decreased H3K4me3 of the human *HOXA9* promoter (**K**), with no change on H3K27me3 (**L**). All ChIP results are normalized to an IgG-matched negative control and enrichment relative to that baseline reported on the *y*-axis. All were $n \geq 3$; Mann–Whitney *t* test: *, $P < 0.05$; **, $P < 0.01$; ***, $P < 0.001$; ±SEM.

shRNA knockdown of *Wdr5* decreased TWIST1-induced cellular stiffness (Supplementary Fig. S7F). We did not observe increased anchorage-independent growth as assayed by soft-agar clonogenicity (Supplementary Fig. S7C) upon shRNA knockdown of *Wdr5* in Myc-CaP-TWIST1 cells. Transcription activator-like effector nuclease (TALEN)-mediated knockout of *WDR5* in PC3-TWIST1 cells (Supplementary Fig. S7G) led to a decreased *HOXA9* expression (Fig. 5D). In addition, loss of *WDR5* resulted in decreased migration potential (Fig. 5E; Supplementary Fig. S7H), invasiveness (Fig. 5F), and resistance to radiation (Supplementary Fig. S7J), but not in soft-agar clonogenicity (Supplementary Fig. S7I) or anoikis resistance (Supplementary Fig. S7K).

In parallel with our results from WDR5 knockdown/knockout, siRNA-mediated knockdown of *Hottip* (Supplementary Fig. S8A), and *HOTTIP* (Supplementary Fig. S8E) in TWIST1-overexpressing Myc-CaP and PC3 cells, respectively, resulted in decreased expression of *Hoxa9*/*HOXA9* (Fig. 5G and J).

Published OnlineFirst May 8, 2017; DOI: 10.1158/0008-5472.CAN-16-2797

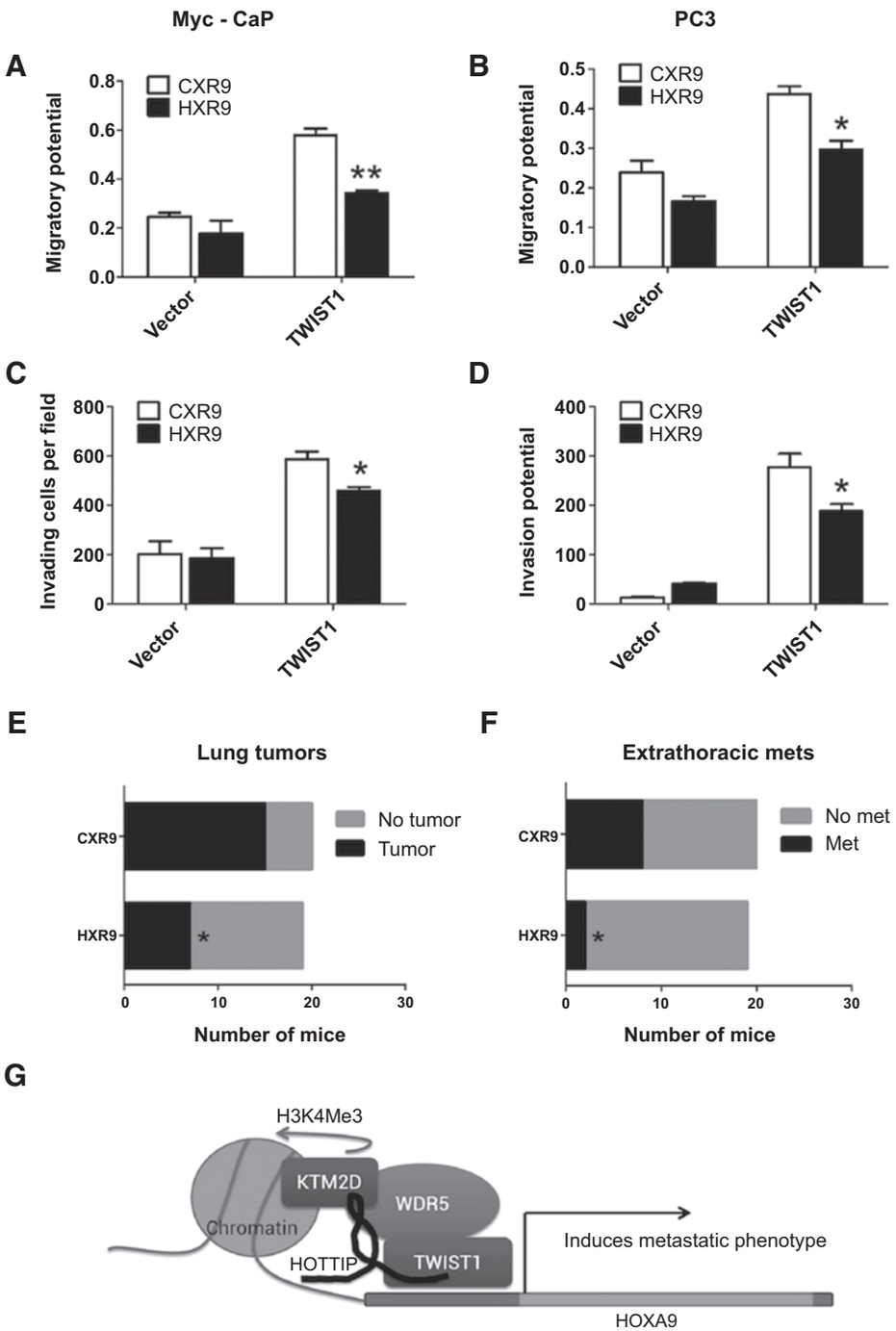

Figure 7.
Pharmacologic inhibition of HOXA9 activity mitigates the prometastatic effects of TWIST1 *in vitro* and *in vivo*. **A** and **C,** Treatment with 10 nmol/L HXR9, a peptide inhibitor of HOXA9, led to decreased cell migration (**A**) and invasion (**C**) compared with the control peptide, CXR9, in Myc-CaP-TWIST1 cells, but not in vector control cells. **B** and **D,** Treatment with 10 nmol/L HXR9 led to a decrease in cell migratory potential (**B**) and invasion (**D**) through Matrigel compared with CXR9 treatment only in PC3-TWIST1 cells and not in PC3 vector control cells. **A–D,** $n \geq 3$; Mann–Whitney *t* test: *, $P < 0.05$; **, $P < 0.01$; ±SEM. **E,** A graph comparing number of athymic nude male mice with macroscopic lung tumors after tail vein injection of Myc-CaP-TWIST1 cells pretreated with HXR9 or CXR9 ($n = 19$–20 mice/arm; *, $P = 0.018$ by Fisher one-sided exact test). **F,** Graph comparing number of athymic nude male mice with presence of at least one extrathoracic metastasis after tail vein injection of Myc-CaP-TWIST1 cells treated with HXR9 or CXR9 ($n = 19$–20 mice/arm; $P = 0.039$ by Fisher one-sided exact test). **G,** Model of a proposed TWIST1–WDR5–*HOTTIP*–KMT2D complex.

Furthermore, knockdown of *Hottip*/*HOTTIP* in Myc-CaP and PC3 cells overexpressing TWIST1, also led to a decrease in migration potential (Fig. 5H and K; and Supplementary Fig. S8B, and S8F) and invasiveness (Fig. 5I and L) but not to an increase in MTC-determined cell stiffness (Supplementary Fig. S8C and S8G) or anoikis resistance (Supplementary Fig. S8D and S8H). All together, these results showed that members of the MLL/COMPASS-like complex, WDR5 and *Hottip*/*HOTTIP*, are partially required for *HOXA9* expression downstream of TWIST1 and the consequent induction of several prometastatic cellular behaviors.

Expression of TWIST1 alters chromatin methylation at the Hoxa9/HOXA9 promoter region

TWIST1 and WDR5 bound directly to the *Hoxa9*/*HOXA9* promoter as shown by chromatin immunoprecipitation (ChIP)

Published OnlineFirst May 8, 2017; DOI: 10.1158/0008-5472.CAN-16-2797

using anti-TWIST1 and anti-WDR5 antibodies coupled with qPCR (ChIP-qPCR) in Myc-CaP and PC3 cells overexpressing TWIST1. Primers flanked E-box sequences, putative TWIST1-binding sites, in the mouse *Hoxa9* (Fig. 6A) as well as the human *HOXA9* promoter region (Fig. 6B). Enrichment of DNA fragments bound by TWIST1 in Myc-CaP and PC3 cells overexpressing TWIST1 are mapped to the *Hoxa9*/*HOXA9* promoter region as shown in Fig. 6A and B and Supplementary Fig. S9B. WDR5 ChIP showed that WDR5 bound to the same regions of the *Hoxa9*/*HOXA9* promoter in Myc-CaP and PC3 cells stably overexpressing TWIST1 (Supplementary Fig. S9A and S9C).

TWIST1 and WDR5 bound together in a complex at the *Hoxa9*/*HOXA9* promoter as shown by primary ChIP followed by secondary immunoprecipitation (re-ChIP) on TWIST1-overexpressing Myc-CaP and PC3 cells. In the ChIP re-ChIP technique, the soluble chromatin fractions derived from cross-linking are divided into two aliquots. The first aliquot was immunoprecipitated with anti-TWIST1 antibody, washed, and the bound antibody–DNA complex was immunoprecipitated with anti-WDR5 antibody (TWIST1> WDR5). The second aliquot was treated identically, except that it was first precipitated with anti-WDR5 antibody followed by re-ChIP with anti-TWIST1 antibody (WDR5>TWIST1). The precipitated DNA was then amplified using primers flanking E-boxes in the mouse *Hoxa9* and human *HOXA9* promoter regions, respectively, as described above. The ChIP re-ChIP experiments showed enrichment of sequences in the *Hoxa9*/*HOXA9* promoter bound by endogenous WDR5 with TWIST1 immunoprecipitates and of TWIST1 bound to WDR5 precipitates in both Myc-CaP and PC3 cells (Fig. 6C and D). This binding was specific as re-ChIP experiments using a nonspecific antibody control did not immunoprecipitate TWIST1 and WDR5 at the same sites on the *Hoxa9*/*HOXA9* promoter in prostate cancer cells overexpressing TWIST1.

We next investigated the mechanism by which the TWIST1–WDR5 complex activated *Hoxa9*/*HOXA9* expression. We found that the epigenetic activation marker, H3K4me3, was enriched in the E-box regions of the *Hoxa9*/*HOXA9* promoter in Myc-CaP and PC3 cells overexpressing TWIST1 by H3K4me3 ChIP (Fig. 6E and G). Interestingly, we also saw enrichment of the repressive histone modification, trimethylation of lysine 27 of histone 3 (H3K27me3), in the *Hoxa9*/*HOXA9* promoter region of TWIST1 stably overexpressing Myc-CaP and PC3 cells (Fig. 6F and H). When we used shRNA-mediated knockdown of *Wdr5* or TALEN-mediated knockout of *WDR5*, we observed abrogated enrichment of the H3K4me3 activation marker in TWIST1-overexpressing Myc-CaP and PC3 cells at the *Hoxa9*/*HOXA9* promoter region (Fig. 6I and K). We did not, however, observe abrogated enrichment of the repressive H3K27me3 marker in the *Hoxa9*/*HOXA9* promoter region in these same cells with reduced or absent WDR5 (Fig. 6J and L). These results showed that TWIST1 binding to the *Hoxa9*/*HOXA9* promoter led to increased H3K4 and H3K27 trimethylation and that WDR5 was required for TWIST1-induced H3K4me3 (activation) but not H3K27me3 (repression) modification of the *Hoxa9*/*HOXA9* promoter region. In summary, our data indicated that TWIST1 and WDR5 bind as a complex to the E-box consensus sequences of the *Hoxa9*/*HOXA9* promoter and promoted *HOXA9* expression that was associated with enrichment of bivalent H3 chromatin markers.

Chemical inhibition of HOXA9 activity mitigates the prometastatic effects of TWIST1 expression

To determine whether this TWIST1–HOXA9 axis could be a potential clinical target, we investigated whether chemical inhibition of HOXA9 or its downstream effectors would decrease the intensity of these prometastatic cellular phenotypes. The effects of two chemical inhibitors of HOXA9 activity were tested. UNC0646 is a small-molecule inhibitor of the methyltransferase G9a that has been shown to inhibit HOXA9 activity in leukemia cells (39), and HXR9 is a peptide inhibitor of HOXA9 that interferes with the interaction of HOXA9 with its cofactor PBX and has been shown to retard the growth of human meningioma (40).

IC_{50} values for each inhibitor were determined for several cell lines including those stably overexpressing TWIST1 (Supplementary Fig. S10), but, in general, we did not see an effect of either agent on cell viability. Treatment of Myc-CaP-TWIST1 and PC3-TWIST1 cells with 250 μmol/L UNC0646 led to decreased migration (Supplementary Fig. S11A and S11C) and invasion (Supplementary Fig. S11B and S11D) compared with vehicle control. Similarly, treatment of Myc-CaP and PC3 cells stably overexpressing TWIST1 with 10 nmol/L HXR9 led to decreased migration (Fig. 7A and B) and invasion (Fig. 7C and D) compared with a scrambled peptide control CXR9. Importantly, these inhibitory effects of UNC0646 and HXR9 were only observed in Myc-CaP and PC3 cells overexpressing TWIST1 and not in isogenic vector control cell lines. These contrasting effects on vector control versus TWIST1-overexpressing cells suggested that HOXA9 inhibition is very specific for TWIST1 overexpression.

To investigate the functional consequences of HOXA9 inhibition in TWIST1-overexpressing cells *in vivo*, we injected Myc-CaP cells incubated with HXR9 or the control peptide, CXR9 into the tail veins of athymic nude mice. We have previously shown that TWIST1 overexpression significantly increased the ability of tail vein–injected Myc-CaP cells to colonize the lungs and form macroscopic metastases as well as extrathoracic metastases in distant subcutaneous tissues, abdominal organs, and distant lymph nodes (6). Thus, TWIST1 allows cells injected into the venous circulation to not only colonize the lungs, but also undergo the full metastatic pathway to produce extrathoracic metastases. We found that TWIST1-overexpressing Myc-CaP cells lost the potential to form macroscopic lung tumors *in vivo* when treated with HXR9 (7/19 mice) as compared with control peptide, CXR9, treated cells (15/20 mice; Fig. 7E, $P = 0.018$ by Fisher exact one-sided test). This trend was also observed with the extrathoracic metastases when Myc-CaP-TWIST1 cells were treated with HXR9 (2/19 mice) as compared with control CXR9 (8/20 mice) treated cells (Fig. 7F, $P = 0.04$ by Fisher exact one-sided test). These results showed that HOXA9 promoted TWIST1-induced metastasis of prostate cancer cells *in vivo* and that pharmacologic HOXA9 inhibition could be a strategy to target TWIST1-induced prostate cancer metastasis.

Discussion

Prostate cancer coopts embryonic developmental programs especially during neoplastic transformation and metastasis as indicated by a significant overlap in differentially expressed genes during prostate development and prostate cancer progression (41). In this study, we show that HOXA9 expression correlates with TWIST1 expression during mouse prostate development. This expression was silenced postnatally in mice; however,

Published OnlineFirst May 8, 2017; DOI: 10.1158/0008-5472.CAN-16-2797

coexpression of TWIST1 and HOXA9 in mouse and human prostate cancer suggests that this developmental mechanism is reactivated during prostate cancer progression. Extending our previous study, which showed that TWIST1 can upregulate HOXA9 expression and that HOXA9 was partially required for TWIST1-mediated EMT phenotypes (6), here we demonstrate that HOXA9 is sufficient for the induction of prometastatic phenotypes alone in prostate cancer cells. Importantly, we show that chemical inhibition of HOXA9 mitigates TWIST1 induction of these prometastatic cellular phenotypes *in vitro* and metastasis *in vivo* implicating HOXA9 as a potential therapeutic target in aggressive and metastatic prostate cancers.

We identify a novel role for TWIST1 in epigenetic regulation of the *Hoxa9*/*HOXA9* locus via interaction with at least two members of the COMPASS-like complex, WDR5 and *Hottip*/*HOTTIP* (Fig. 7G). In corroboration with a previous study from another group (37), we show that TWIST1 binds to WDR5, an invariant component of the COMPASS-like complexes. Importantly, we demonstrated the novel finding that TWIST1 also binds to the lncRNA *Hottip*/*HOTTIP* that recruits and directs the COMPASS-like complex to the *Hox*/*HOX* cluster (24). Furthermore, both WDR5 and *Hottip*/*HOTTIP* are required to observe the full potential of TWIST1-induced *HOXA9* expression and acquisition of prometastatic properties in prostate cancer cells. Overexpression of *HOTTIP* and subsequent *HOX* gene expression has been associated with poor prognosis and increased aggressiveness in other cancers (42–44). The common overexpression of the WDR5–*HOTTIP* complex across multiple types of cancer suggests that it is a key pathway in cancer progression and targeting this pathway successfully may have the potential to benefit many cancer patients. Our new findings also extend the catalog of protein targets for aggressive TWIST1 and MLL/COMPASS-driven prostate cancer to include HOXA9. TWIST1 and HOXA9 were important for metastatic phenotypes in both AR-dependent and AR-independent models, suggesting that this TWIST1-COMPASS-like–HOXA9 axis can function independently of the AR axis.

TWIST1 as a transcription factor directly activates and represses the transcription of target genes, but there is evidence to suggest that TWIST1 also has broad epigenetic effects. TWIST1 can interact with SET8, leading to H4K20 monomethylation and target gene expression (45). TWIST1 led to a 2-fold genome-wide increase in the number of TWIST1 target genes with bivalent chromatin configurations (36) rendering gene promoters poised for activation (46) and facilitating increased cellular plasticity that is characteristic of EMT (36). Herein, we have uncovered a mechanistic role for TWIST1 in directly targeting the COMPASS-like HMT complex to the *Hoxa9*/*HOXA9* promoter, resulting in alteration of chromatin methylation patterns in prostate cancer cells. Overexpression of TWIST1 led to an increase in both H3K4 and H3K27 trimethlyation at the *Hoxa9*/*HOXA9* promoter region, consistent with a bivalent chromatin configuration. Intriguingly, knockdown of WDR5 in the presence of TWIST1 abrogates the increase in H3K4 trimethylation, but not H3K27 trimethylation. These observations are consistent with TWIST1 cooperating with WDR5 and the whole COMPASS-like complex to increase H3K4 trimethylation at the *Hoxa9*/*HOXA9* promoter region and thereby upregulate *Hoxa9*/*HOXA9* expression. However, the presence of concurrent increased H3K27 trimethylation indicates the possible presence of additional chromatin-regulatory mechanisms interacting with TWIST1, such as the Polycomb-repressive complexes.

In conclusion, this study demonstrates a novel mechanistic role of TWIST1 in promoting prostate cancer aggressiveness not only by direct transcriptional activation of *Hoxa9*/*HOXA9* but also by epigenetic reprogramming of the *Hoxa9*/*HOXA9* locus. In addition to its documented functions as a direct transcriptional activator and repressor, TWIST1 cooperates with the COMPASS-like HMT complex to directly increase H3K4me3 in the promoter region of *Hoxa9*/*HOXA9*. TWIST1 and HOXA9 appear to direct an embryonic developmental program for prostate organogenesis that is reactivated during prostate cancer metastasis. Importantly, therapeutic targeting of HOXA9 is sufficient to abrogate TWIST1-induced prostate cancer metastasis. Our findings are consistent with the concept that targeting epithelial plasticity programs in advanced prostate cancer is an area that should be studied more preclinically (47) with an eye toward future clinical translation.

Disclosure of Potential Conflicts of Interest

No potential conflicts of interest were disclosed.

Authors' Contributions

Conception and design: R. Malek, R.P. Gajula, R.D. Williams, P.T. Tran
Development of methodology: R. Malek, R.P. Gajula, R.D. Williams, H. Wang, S.S. An, P.T. Tran
Acquisition of data (provided animals, acquired and managed patients, provided facilities, etc.): R. Malek, R.P. Gajula, R.D. Williams, B. Nghiem, B.W. Simons, K. Nugent, K. Taparra, G. Lemtiri-Chlieh, L. True, S.S. An, A.E. Ross, P.J. Hurley, C. Morrissey, P.T. Tran
Analysis and interpretation of data (e.g., statistical analysis, biostatistics, computational analysis): R. Malek, R.P. Gajula, R.D. Williams, B.W. Simons, H. Wang, S.S. An, E.M. Schaeffer, K.J. Pienta, P.J. Hurley, C. Morrissey, P.T. Tran
Writing, review, and/or revision of the manuscript: R. Malek, R.P. Gajula, R.D. Williams, B. Nghiem, B.W. Simons, H. Wang, G. Lemtiri-Chlieh S.S. An, T.L. DeWeese, A.E. Ross, E.M. Schaeffer, K.J. Pienta, P.J. Hurley, C. Morrissey, P.T. Tran
Administrative, technical, or material support (i.e., reporting or organizing data, constructing databases): R. Malek, R.D. Williams, G. Lemtiri-Chlieh, A.R. Yoon, L. True, S.S. An, E.M. Schaeffer, P.T. Tran
Study supervision: R. Malek, P.T. Tran

Acknowledgments

We thank the patients and their families who were willing to participate in the University of Washington Prostate Cancer Donor Program and investigators Drs. Robert Vessella, Celestia Higano, Bruce Montgomery, Evan Yu, Peter Nelson, Heather Cheng, Paul Lange, and Martine Roudier.

Grant Support

R.D. Williams was a Johns Hopkins Laboratory Radiation Oncology Training Fellow (supported by NIH-T32CA121937). K. Taparra was funded by the NIH (F31CA189588). H.L. Wang is funded by a Uniting Against Lung Cancer Young Investigator Award. S.S. An was funded by the NIH (P50CA103175, U54CA141868 and HL107361). P.T. Tran is funded by the Motta and Nesbitt Families, the DoD (W81XWH-11-1-0272), a Kimmel Translational Science Award (SKF-13-021), an ACS Scholar award (122688-RSG-12-196-01-TBG), American Lung Association (LCD-339465), Movember-PCF and the NIH (R01CA166348 and U01CA183031). L. True and C. Morrissey were funded by the Pacific Northwest CaP SPORE (P50CA97186) and the Richard M. Lucas Foundation.

The costs of publication of this article were defrayed in part by the payment of page charges. This article must therefore be hereby marked *advertisement* in accordance with 18 U.S.C. Section 1734 solely to indicate this fact.

Received October 27, 2016; revised March 3, 2017; accepted April 19, 2017; published OnlineFirst May 8, 2017.

Published OnlineFirst May 8, 2017; DOI: 10.1158/0008-5472.CAN-16-2797

References

1. Siegel RL, Miller KD, Jemal A. Cancer statistics, 2016. CA Cancer J Clin 2016;66:7–30.
2. Pound CR, Partin AW, Eisenberger MA, Chan DW, Pearson JD, Walsh PC. Natural history of progression after PSA elevation following radical prostatectomy. JAMA 1999;281:1591–7.
3. Kwok WK, Ling M-T, Lee T-W, Lau TCM, Zhou C, Zhang X, et al. Up-regulation of TWIST in prostate cancer and its implication as a therapeutic target. Cancer Res 2005;65:5153–62.
4. Shiota M, Yokomizo A, Tada Y, Inokuchi J, Kashiwagi E, Masubuchi D, et al. Castration resistance of prostate cancer cells caused by castration-induced oxidative stress through Twist1 and androgen receptor overexpression. Oncogene 2010;29:237–50.
5. Gajula RP, Chettiar ST, Williams RD, Nugent K, Kato Y, Wang H, et al. Structure-function studies of the bHLH phosphorylation domain of TWIST1 in prostate cancer cells. Neoplasia 2015;17:16–31.
6. Gajula RP, Chettiar ST, Williams RD, Thiyagarajan S, Kato Y, Aziz K, et al. The twist box domain is required for twist1-induced prostate cancer metastasis. Mol Cancer Res 2013;1541–7786.
7. Krumlauf R. Hox genes in vertebrate development. Cell 1994;78:191–201.
8. Noordermeer D, Leleu M, Splinter E, Rougemont J, De Laat W, Duboule D. The dynamic architecture of Hox gene clusters. Science 2011;334:222–5.
9. Bhatlekar S, Fields JZ, Boman BM. HOX genes and their role in the development of human cancers. J Mol Med 2014;92:811–23.
10. Collins CT, Hess JL. Role of HOXA9 in leukemia: dysregulation, cofactors and essential targets. Oncogene 2016;35:1090–8.
11. Soshnikova N, Duboule D. Epigenetic temporal control of mouse Hox genes *in vivo*. Science 2009;324:1320–3.
12. Li A, Yang Y, Gao C, Lu J, Jeong H-W, Liu BH, et al. A SALL4/MLL/HOXA9 pathway in murine and human myeloid leukemogenesis. J Clin Invest 2013;123:4195–207.
13. Shilatifard A.The COMPASS family of histone H3K4 methylases: mechanisms of regulation in development and disease pathogenesis. Annu Rev Biochem 2012;81:65–95.
14. Döhner K, Tobis K, Ulrich R, Fröhling S, Benner A, Schlenk RF, et al. Prognostic significance of partial tandem duplications of the MLL gene in adult patients 16 to 60 years old with acute myeloid leukemia and normal cytogenetics: a study of the Acute Myeloid Leukemia Study Group Ulm. J Clin Oncol 2002;20:3254–61.
15. Kandoth C, McLellan MD, Vandin F, Ye K, Niu B, Lu C, et al. Mutational landscape and significance across 12 major cancer types. Nature 2013;502:333–9.
16. Grasso CS, Wu Y-M, Robinson DR, Cao X, Dhanasekaran SM, Khan AP, et al. The mutational landscape of lethal castration-resistant prostate cancer. Nature 2012;487:239–43.
17. Malik R, Khan AP, Asangani IA, Cies´lik M, Prensner JR, Wang X, et al. Targeting the MLL complex in castration-resistant prostate cancer. Nat Med 2015;21:344–52.
18. Tran PT, Shroff EH, Burns TF, Thiyagarajan S, Das ST, Zabuawala T, et al. Twist1 suppresses senescence programs and thereby accelerates and maintains mutant kras-induced lung tumorigenesis. PLoS Genet 2012;8:e1002650.
19. Tran PT, Fan AC, Bendapudi PK, Koh S, Komatsubara K, Chen J, et al. Combined inactivation of MYC and K-Ras oncogenes reverses tumorigenesis in lung adenocarcinomas and lymphomas. PLoS One 2008;3:e2125.
20. Zeng J, See AP, Aziz K, Thiyagarajan S, Salih T, Gajula RP, et al. Nelfinavir induces radiation sensitization in pituitary adenoma cells. Cancer Biol Ther 2011;12:657–63.
21. Fiucci G, Ravid D, Reich R, Liscovitch M. Caveolin-1 inhibits anchorage-independent growth, anoikis and invasiveness in MCF-7 human breast cancer cells. Oncogene 2002;21:2365–75.
22. An SS, Fabry B, Trepat X, Wang N, Fredberg JJ. Do biophysical properties of the airway smooth muscle in culture predict airway hyperresponsiveness? Am J Respir Cell Mol Biol 2006;35:55–64.
23. Fabry B, Maksym GN, Butler JP, Glogauer M, Navajas D, Fredberg JJ. Scaling the microrheology of living cells. Phys Rev Lett 2001;87:148102.
24. Wang KC, Yang YW, Liu B, Sanyal A, Corces-Zimmerman R, Chen Y, et al. A long noncoding RNA maintains active chromatin to coordinate homeotic gene expression. Nature 2011;472:120–4.
25. Zeisig BB, Milne T, García-Cuéllar M-P, Schreiner S, Martin M-E, Fuchs U, et al. Hoxa9 and Meis1 are key targets for MLL-ENL-mediated cellular immortalization. Mol Cell Biol 2004;24:617–28.
26. Takeda A, Goolsby C, Yaseen NR. NUP98-HOXA9 induces long-term proliferation and blocks differentiation of primary human CD34+ hematopoietic cells. Cancer Res 2006;66:6628–37.
27. Huang L, Pu Y, Hepps D, Danielpour D, Prins GS. Posterior Hox gene expression and differential androgen regulation in the developing and adult rat prostate lobes. Endocrinology 2007;148:1235–45.
28. Shiota M, Yokomizo A, Tada Y, Inokuchi J, Kashiwagi E, Masubuchi D, et al. Castration resistance of prostate cancer cells caused by castration-induced oxidative stress through Twist1 and androgen receptor overexpression. Oncogene 2010;29:237–50.
29. Hurwitz AA, Foster BA, Allison JP, Greenberg NM, Kwon ED. The TRAMP mouse as a model for prostate cancer. Curr Protoc Immunol 2001;20:20.5.
30. Ellwood-Yen K, Graeber TG, Wongvipat J, Iruela-Arispe ML, Zhang J, Matusik R, et al. Myc-driven murine prostate cancer shares molecular features with human prostate tumors. Cancer Cell 2003;4:223–38.
31. Wang S, Gao J, Lei Q, Rozengurt N, Pritchard C, Jiao J, et al. Prostate-specific deletion of the murine Pten tumor suppressor gene leads to metastatic prostate cancer. Cancer Cell 2003;4:209–21.
32. Bruxvoort KJ, Charbonneau HM, Giambernardi TA, Goolsby JC, Qian C-N, Zylstra CR, et al. Inactivation of Apc in the mouse prostate causes prostate carcinoma. Cancer Res 2007;67:2490–6.
33. Taylor BS, Schultz N, Hieronymus H, Gopalan A, Xiao Y, Carver BS, et al. Integrative genomic profiling of human prostate cancer. Cancer Cell 2010;18:11–22.
34. Cerami E, Gao J, Dogrusoz U, Gross BE, Sumer SO, Aksoy BA, et al. The cBio cancer genomics portal: an open platform for exploring multidimensional cancer genomics data. Cancer Discov 2012;2:401–4.
35. Gao J, Aksoy BA, Dogrusoz U, Dresdner G, Gross B, Sumer SO, et al. Integrative analysis of complex cancer genomics and clinical profiles using the cBioPortal. Sci Signal 2013;6:pl1.
36. Malouf GG, Taube JH, Lu Y, Roysarkar T, Panjarian S, Estecio MR, et al. Architecture of epigenetic reprogramming following Twist1-mediated epithelial-mesenchymal transition. Genome Biol 2013;14:R144.
37. Wu M-Z, Tsai Y-P, Yang M-H, Huang C-H, Chang S-Y, Chang C-C, et al. Interplay between HDAC3 and WDR5 is essential for hypoxia-induced epithelial-mesenchymal transition. Mol Cell 2011;43:811–22.
38. Song J-J, Kingston RE. WDR5 interacts with mixed lineage leukemia (MLL) protein via the histone H3-binding pocket. J Biol Chem 2008;283:35258–64.
39. Lehnertz B, Pabst C, Su L, Miller M, Liu F, Yi L, et al. The methyltransferase G9a regulates HoxA9-dependent transcription in AML. Genes Dev 2014;28:317–27.
40. Ando H, Natsume A, Senga T, Watanabe R, Ito I, Ohno M, et al. Peptide-based inhibition of the HOXA9/PBX interaction retards the growth of human meningioma. Cancer Chemother Pharmacol 2014;73:53–60.
41. Schaeffer E, Marchionni L, Huang Z, Simons B, Blackman A, Yu W, et al. Androgen-induced programs for prostate epithelial growth and invasion arise in embryogenesis and are reactivated in cancer. Oncogene 2008;27:7180–91.
42. Quagliata L, Matter MS, Piscuoglio S, Arabi L, Ruiz C, Procino A, et al. lncRNA HOTTIP/HOXA13 expression is associated with disease progression and predicts outcome in hepatocellular carcinoma patients. Hepatol 2014;59:911–23.
43. Sang Y, Zhou F, Wang D, Bi X, Liu X, Hao Z, et al. Up-regulation of long non-coding HOTTIP functions as an oncogene by regulating HOXA13 in non-small cell lung cancer. Am J Transl Res 2016;8:2022–32.

Published OnlineFirst May 8, 2017; DOI: 10.1158/0008-5472.CAN-16-2797

44. Li Z, Zhao X, Zhou Y, Liu Y, Zhou Q, Ye H, et al. The long non-coding RNA HOTTIP promotes progression and gemcitabine resistance by regulating HOXA13 in pancreatic cancer. J Transl Med 2015;13:84
45. Yang F, Sun L, Li Q, Han X, Lei L, Zhang H, et al. SET8 promotes epithelial–mesenchymal transition and confers TWIST dual transcriptional activities. EMBO J 2012;31:110–23.
46. Bernstein BE, Mikkelsen TS, Xie X, Kamal M, Huebert DJ, Cuff J, et al. A bivalent chromatin structure marks key developmental genes in embryonic stem cells. Cell 2006;125:315–26.
47. Ware KE, Somarelli JA, Schaeffer D, Li J, Zhang T, Park S, et al. Snail promotes resistance to enzalutamide through regulation of androgen receptor activity in prostate cancer. Oncotarget 2016;7:50507–21.

Cancer Research
The Journal of Cancer Research (1916–1930) | The American Journal of Cancer (1931–1940)

AACR American Association for Cancer Research

TWIST1-WDR5-*Hottip* Regulates *Hoxa9* Chromatin to Facilitate Prostate Cancer Metastasis

Reem Malek, Rajendra P. Gajula, Russell D. Williams, et al.

Cancer Res 2017;77:3181-3193. Published OnlineFirst May 8, 2017.